Research Article Vol. 57, No. 14 / 10 May 2018 / Applied Optics 3639

applied optics

Design of an ultrasensitive SPR biosensor based on a graphene-MoS_2 hybrid structure with a MgF_2 prism

Yuncai Feng,[1,2] Youwen Liu,[1,*] and Jinghua Teng[2]

[1]Department of Applied Physics, Nanjing University of Aeronautics and Astronautics, Nanjing 210016, China
[2]Institute of Materials Research and Engineering, Agency for Science, Technology and Research (A*STAR), 2 Fusionopolis Way, Singapore 138634, Singapore
*Corresponding author: ywliu@nuaa.edu.cn

Received 31 January 2018; revised 7 April 2018; accepted 11 April 2018; posted 12 April 2018 (Doc. ID 321176); published 2 May 2018

We propose, to the best of our knowledge, a new configuration of a biosensor based on the graphene-MoS_2 hybrid structure by adopting the lower refractive index MgF_2 prism in order to improve the sensitivity and the figure of merit (FOM). We can obtain an ultrasensitive sensor with values of sensitivity and FOM as high as 540.8°/RIU and 145/RIU, respectively, by modulating the parameters in the configuration and comparatively choosing a different absentee layer material. The proposed structure is applicable in the realization of an integrated device for the surface plasmon resonance biosensor.

OCIS codes: (130.6010) Sensors; (240.6680) Surface plasmons.

https://doi.org/10.1364/AO.57.003639

1. INTRODUCTION

Surface plasmon polaritons (SPPs) are the localized surface electromagnetic waves propagating along the metal/dielectric interface and evanescently confined in the perpendicular direction [1]. The SPPs will be excited by the light beam whose in-plane wave vector matches the wave vector of SPPs; meanwhile, the surface plasmon resonance (SPR) will be realized around the interface. Once the SPR is excited, the energy will be transferred from the photon to the SPPs, and it would result in an enormous decrease of the reflectance. Based on this principle, different kinds of plasmonic sensors [2–8] were designed in previous years.

SPR sensors offer many advantages such as high sensitivity [8–12], real-time dynamic detection, and the making of the samples with no mark. Many innovative techniques have been reported to enhance the performance of sensors. Abdulhalim *et al.* presented a method that adds a high index layer on a metal layer to improve the sensitivity [10]. Verma *et al.* have proved theoretically that the addition of a semiconductor (Si) layer between the metal and graphene layers enhances the performance of SPR biosensors [13]. Ouyang *et al.* designed an SPR biosensor structure based on silicon nanosheet and two-dimensional transition metal dichalcogenides (TMDCs) [14]. However, in order to meet the ever-increasing demands in industrial processes, excellent and higher sensitivity sensors are expected.

In recent years, graphene has attracted the attention of many scholars for its distinctive optical and electrical properties [15]. It has been applied to many fields, such as plasmonic filters [16,17], optical modulators [18], tunable intersection structures [19], beam splitters [20], and sensors [21,22]. In SPR biosensors, Wu *et al.* presented a sensor based on graphene-on-gold where the additional graphene layer greatly improves sensitivity compared to the conventional metal SPR sensor [4]. More recently, another two-dimensional material MoS_2 that belongs to TMDCs is known as "beyond graphene" nanomaterial, and it is extensively used in sensor fields. In addition, the graphene-MoS_2 hybrid structure [23–25] is used for achieving excellent sensors. In a graphene-MoS_2 hybrid nanostructure, the MoS_2 layer can provide enough excitation energy for effective charge transfer. In addition, the deep reflectance dip can be obtained, as the MoS_2 layer possesses high optical absorption efficiency (~5%).

In this work, we propose an ultrasensitive SPR biosensor based on a graphene-MoS_2 hybrid structure with a low refractive index MgF_2 prism. We deduce that an ultrahigh sensitivity and figure-of-merit (FOM) sensor can be realized, and the sensitivity may arrive at 540.8°/RIU. In addition, the parameters in the configuration for the best optimization results are also clarified. We believe that the structure could find potential applications in gas detection, medical diagnosis, and biosensors.

2. MODELS AND NUMERICAL METHODS

The high-sensitivity biosensor based on a graphene-MoS_2 hybrid structure is presented, as shown in Fig. 1. The MgF_2 prism

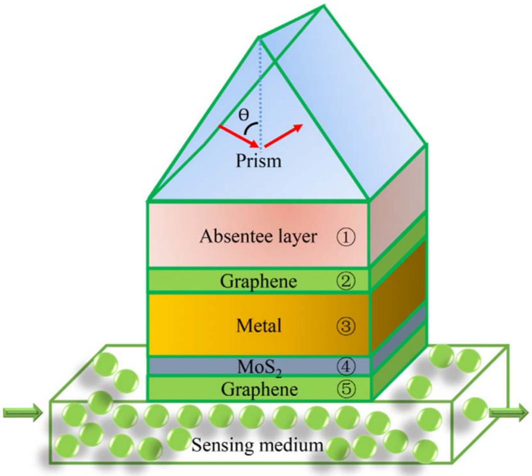

Fig. 1. Schematic diagram of the biosensor based on a graphene-MoS_2 hybrid structure with MgF_2 prism.

is employed to realize the sensing probe experimentally; here the refractive index of the prism is 1.377 at $\lambda = 632.8$ nm [26]. In the previous study, Maharana *et al.* [27] designed an SPR biosensor with high sensitivity by utilizing air gap between prism and gold film to enhance the sensitivity. Likewise, here an absentee layer between the prism and metal film is used to improve the sensitivity. In the structure, it contains five layers of thin film. The first layer is the absentee layer, and air, silicon dioxide, potassium chloride, silicon nitride, titanium dioxide, and lead sulfide can be chosen as the absentee layer, and the refractive index at wavelength 632.8 nm is 1, 1.457 [28], 1.487 [29], 2.02 [29], 2.5837 [28], 3.92 [29], respectively. The second layer is the graphene layer, which can prevent the metal layer from being oxidized, and the complex refractive index in the visible range is given as [30]

$$n_2 = 3.0 + i\frac{C}{3}\lambda, \tag{1}$$

where the λ is the wavelength of incident light in μm and the constant $C \approx 5.446\ \mu m^{-1}$. The thickness of graphene is $d_2 = 0.34$ nm.

In the metal layer, the Al film is chosen as the SPR metal because it exhibits excellent dispersion characteristics. The complex refractive index is calculated through the Drude–Lorentz model,

$$n_3 = \sqrt{1 - \frac{\lambda^2 \lambda_c}{\lambda_p^2(\lambda_c + i\lambda)}}, \tag{2}$$

where λ is the wavelength in μm, and λ_p and λ_c represent the plasma wavelength and collision wavelength whose values are 1.0657×10^{-7} m, 2.451×10^{-5} m, respectively.

In addition, the fourth layer and fifth layer are a graphene-MoS_2 hybrid nanostructure, in the structure; the MoS_2 layer has a much higher optical absorption coefficient (∼5%) than the graphene layer, so it will lead to a significant effect of SPR signals. In addition, the graphene layer can capture the target biomolecules through pi-stacking force. The refractive index of MoS_2 at $\lambda = 632.8$ nm is 5.9 + 0.8i [31], and the thickness is $d_4 = 0.65$ nm.

The sensing medium is deionized (DI) water, and its refractive index is given as [32]

$$n_6 = \sqrt{\sum_1^4 \frac{A_i \lambda^2}{\lambda^2 - t_i^2} + 1}, \tag{3}$$

where the Sellmeier coefficients $A_1 = 5.667 \times 10^{-1}$, $A_2 = 1.732 \times 10^{-1}$, $A_3 = 2.096 \times 10^{-2}$, $A_4 = 1.125 \times 10^{-1}$, $t_1 = 5.084 \times 10^{-3}$, $t_2 = 1.818 \times 10^{-2}$, $t_3 = 2.625 \times 10^{-2}$, $t_4 = 1.074 \times 10^1$, and the wavelength in μm.

To theoretically investigate the sensitivity of the SPR biosensor, we employed the transfer matrix method (TMM) [3,4]. It is considered that all the layers are optically isotropic and nonmagnetic. Now the field at the first boundary and at the last boundary can be given as

$$\begin{bmatrix} E_1 \\ H_1 \end{bmatrix} = M \begin{bmatrix} E_N \\ H_N \end{bmatrix}, \tag{4}$$

where M is the total characteristic matrix. It is noted that the SPP modes are p-polarization, for the p-polarization light M is written as [22]

$$M = \prod_{j=1}^{j=N} M_j = \begin{bmatrix} M_{11} & M_{12} \\ M_{21} & M_{22} \end{bmatrix}, \tag{5}$$

with

$$M_j = \begin{bmatrix} \cos\beta_j & (-i\sin\beta_j)/q_j \\ -iq_j\sin\beta_j & \cos\beta_j \end{bmatrix}, \tag{6}$$

where

$$q_j = \frac{\sqrt{\varepsilon_j - n_0^2\sin^2\theta}}{\varepsilon_j}; \tag{7}$$

here, N, ε_j, and θ are the number of the layers in the stack $N = 5$, the dielectric constant, and the incident angle. The total reflection coefficient for p-polarization is given as

$$r = \frac{(M_{11} + M_{12}q_N)q_1 - (M_{21} + M_{22}q_N)}{(M_{11} + M_{12}q_N)q_1 + (M_{21} + M_{22}q_N)}, \tag{8}$$

and the total reflectance for p-polarization light is given as

$$R = |r|^2. \tag{9}$$

Since the reflectance significantly varies with the change in the refractive index of the sensing medium, the large shift in the reflectance would lead to a high sensitivity. If the refractive index of the sensing layer is altered by Δn_s, and the corresponding shift in the resonance angle is $\Delta\theta_r$, the sensitivity of SPR biosensor is defined as follows:

$$S = \frac{\Delta\theta_r}{\Delta n_s}. \tag{10}$$

In addition, the full width at half-maximum (FWHM) corresponding to the reflectance curves should be as small as possible so that the error in determining the signal is minimum. Thus, in order to describe the performance of the SPR sensor, the FOM is defined as follows:

$$\mathrm{FOM} = \frac{S}{\mathrm{FWHM}}. \tag{11}$$

3. NUMERICAL RESULTS AND DISCUSSION

First, the laser source with 632.8 nm wavelength is supposed to be the light source for the SPR biosensor. The refractive index of the sensing medium is given as $n_s = 1.332 + \Delta n_s$, where Δn_s is the change in the refractive index of the sensing medium. Besides, the initial thickness of the absentee layer is set to 10 nm, and the optimized thickness of Al thin film is 30 nm, which can obtain a deep reflectance dip. As shown in Fig. 2, the performances of three SPR sensors are presented, where the structures are metal-MoS_2-graphene, graphene-metal-MoS_2-graphene, and silicon dioxide-graphene-metal-MoS_2-graphene, respectively. In our calculations, the change in refractive index of sensing medium $\Delta n_s = 0.005$, and the number of the graphene layer and MoS_2 are one. As shown in Fig. 2, it is found that the shift of the dip in reflectance spectra is the largest as the introduction of the silicon dioxide absentee layer with the graphene-MoS_2 hybrid structure.

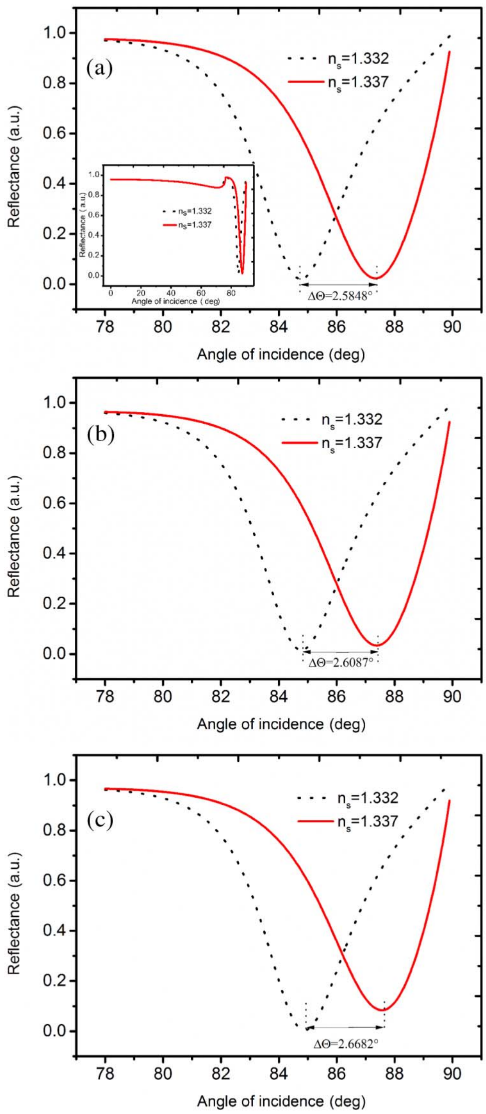

Fig. 2. Variation of the reflectance with three kinds of different SPR sensors; (a) metal-MoS_2-graphene (the illustration shows the result in all situations); (b) graphene-metal-MoS_2-graphene; (c) silicon dioxide-graphene-metal-MoS_2-graphene.

Table 1. Performance Comparisons of SPR Sensor with Common Materials

Absentee Layer	Resonance Angle (°)	Sensitivity (°/RIU)	FWHM (°)	FOM (RIU^{-1})
Air	83.956	324.004	5.165	62.736
SiO_2	84.897	533.654	3.665	145.600
KCl	84.933	536.036	3.689	145.307
Si_3N_4	85.326	514.595	3.522	146.079
TiO_2	85.493	478.859	3.511	136.408
PbS	85.659	435.975	3.594	121.313

Table 1 lists the main performance parameters (sensitivity and FOM) of the SPR sensor with an absentee layer (different common materials) in initial structure. As shown in Table 1, the sensor with the potassium chloride absentee layer can achieve the highest sensitivity $S = 536.036°/\mathrm{RIU}$. Owing to the approximately equal FOM in the SPR sensor with different absentee layers (silicon dioxide, potassium chloride, and silicon nitride), the absentee layer with the highest sensitivity is selected to design the best SPR biosensor; that is, the potassium chloride is chosen as the absentee layer.

The variation of sensitivity of our proposed structure is plotted in Fig. 3. In our simulation, the thickness of the absentee layer is optimized by keeping the thickness of other layers fixed. As shown in Fig. 3, the sensitivity of the SPR biosensor increases first and then decreases with the increase of the thickness of the absentee layer. When the thickness of the absentee layer is up to 16 nm, the sensitivity of the SPR sensor reaches a maximum $S = 540.8°/\mathrm{RIU}$; thus, we set the thickness of the absentee layer in the proposed structure as $d_1 = 16$ nm.

To further optimize the sensitivity of the proposed sensor, the number of the graphene layer is discussed by using the numerical simulation method. As we know, the second layer graphene is presented to prevent the metal layer from being oxidized from the absentee layer; thus, this graphene layer may be treated as the part of the absentee layer. When the optimization of the thickness of the absentee layer is fixed, the sensitivity of the structure will decrease with the increasing

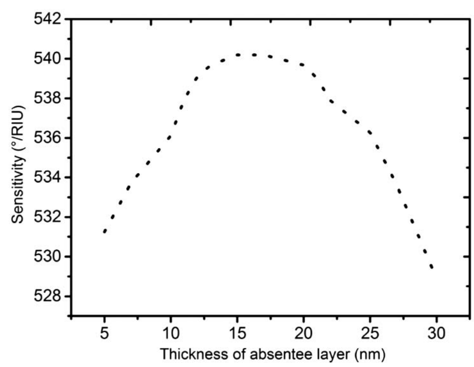

Fig. 3. Optimization of the thickness of the potassium chloride absentee layer.

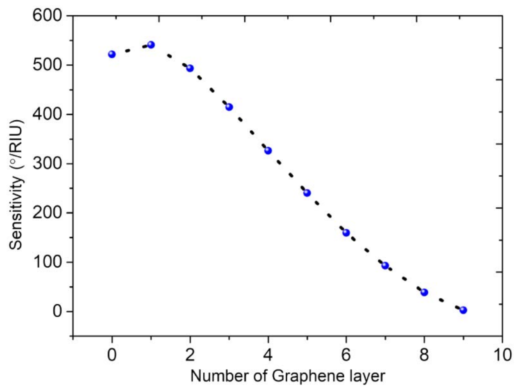

Fig. 4. Variation of sensitivity in accordance with the number of the graphene layer (the fifth layer).

number of the second layer graphene, so it does not merit any additional discussion. However, the fifth layer graphene does not belong to the absentee layer, and it may have effects on sensitivity.

As shown in Fig. 4, the variation of sensitivity in accordance with the number of the graphene layer (the fifth layer) is presented. When the number of the fifth layer graphene $L = 0$, it represents the sensing medium's direct contact with the MoS_2 layer. From the figure, it can be found that the sensor has the highest sensitivity when the number of graphene layer $L = 1$, and the sensitivity gradually decreases with the increasing number of the graphene layer; thus, the number of the graphene layer in the proposed structure is set as $L = 1$. Besides, the thickness of metal is an important parameter for the performance of the SPR sensor; in fact, we found that the sensitivity increases first and then decreases with the increasing of metal thickness, and when the thickness of metal layer $d = 30$ nm, the sensitivity reaches maximum $S = 540.8°/\mathrm{RIU}$. Therefore, the thickness of metal layer $d = 30$ nm is the best choice to design this kind of sensor.

In addition, the reflectance as a function of incident angle for a different number of MoS_2 layers is plotted in Fig. 5. The result shows that the SPR curves become broader with the increasing number of MoS_2 layers. Moreover, by numerical calculations, it is found that the value of sensitivity declines sharply as the number of MoS_2 layers increases. The value of sensitivity is $S = 540.8°/\mathrm{RIU}$ when the number of MoS_2 layer $N = 1$, and the value of sensitivity is $S = 112.0°/\mathrm{RIU}$ when the number of MoS_2 layer $N = 3$. Besides, even there is not an MoS_2 layer, the value of sensitivity is still small. Therefore, the number of MoS_2 $N = 1$ is the best choice to design this kind of SPR biosensor.

Finally, the optimum design is presented; the configuration is composed of the MgF_2 prism, a potassium chloride absentee layer with 16 nm thickness, a single graphene sheet, Al thin film with 30 nm thickness, a single MoS_2 sheet, and monolayer graphene. Such a system can be implemented by the method of deposit and transfer.

It is known that the SP field distribution at the sensing medium interface largely affects the overall performance of the SPR sensor through the overlap integral between the

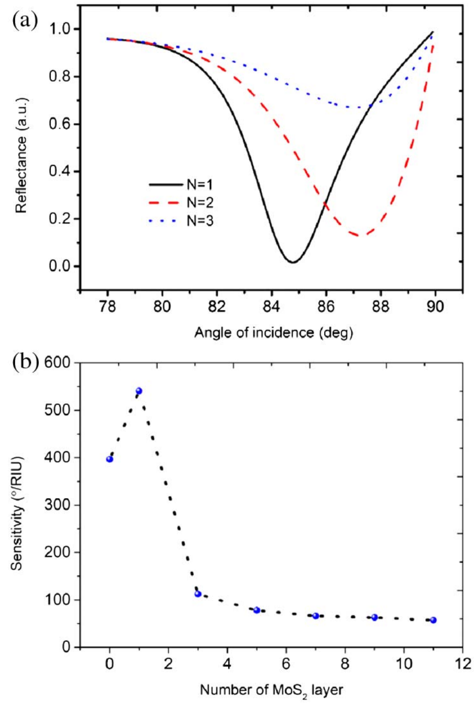

Fig. 5. Optimization of the thickness of the MoS_2 layer. (a) The reflectance as a function of the angle of incidence for a different number of MoS_2 layers. (b) The sensitivity as the function of the number of MoS_2 layers.

evanescent field and the distribution of the dielectric constant of the sensing layer [33]. Enhancing the field at the sensing medium interface is a good approach to increase the sensitivity of the SPR biosensor. We investigate the filed distribution of the proposed structure by using the finite-difference time-domain (FDTD) method with a perfect matched layer (PML) as the absorbing condition. As shown in Fig. 6(a), the field intensity as a function of the distance from the prism interface for the optimum design configuration is illustrated. Meanwhile, the 3D profiles of electric field distributions are also shown in Fig. 6(b). Obviously, the electric field of the evanescent wave is enormously magnified in the graphene-MoS_2 hybrid layer, and thus the sensitivity is largely enhanced. Besides, the sensitivity as a function of the refractive index of the prism is illustrated in Fig. 6(c), and one can see that the sensitivity decreases with the increasing refractive index of the prism. Similarly, the filed distributions are displayed in the structure with a different refractive index of the prism, and the SP field is the largest at the sensing medium interface with the use of the MgF_2 prism, which leads to the highest sensitivity. In fact, we also can explain the result by using the resonance condition $n_{\mathrm{prism}} \sin\theta_r = \mathrm{Re}(n_2)$, where $\mathrm{Re}(n_2)$ is the real part of the effective index of the configuration behind the prism, and it may be expressed as function $\mathrm{Re}(n_2) = f(n_s)$ of the refractive index n_s of the sensing medium. Obviously, the lower the refractive index n_s of the used prism, the larger the resonance angle $\theta_r (< \pi/2)$. By directly differentiating the above expression, the sensitivity is given by $\Delta\theta_r/\Delta n_s = f'(n_s)/n_{\mathrm{prism}} \cos\theta_r$. From the formula,

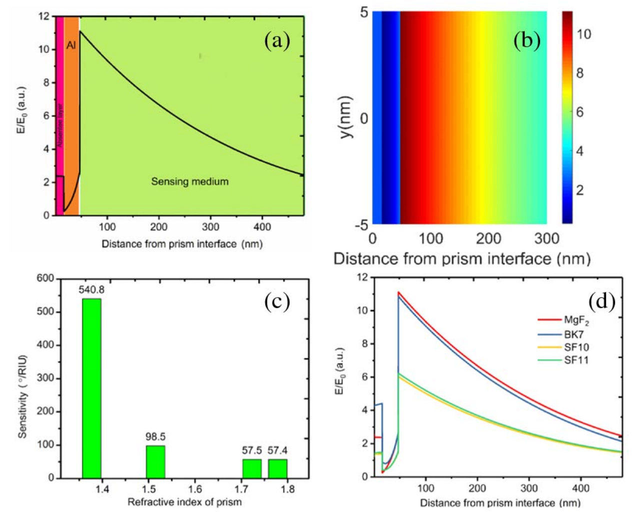

Fig. 6. (a) Field intensity as a function of the distance from prism interface for the optimum design configuration; (b) the 3D profile of the electric field distribution; (c) the sensitivity as a function of the refractive index of prism; (d) the field intensity as a function of the distance from prism interface in the configuration with different prisms at resonance condition for MgF_2 prism $\theta_r = 85.02°$, BK7 prism $\theta_r = 65.32°$, SF10 prism $\theta_r = 53.09°$, and SF11 prism $\theta_r = 50.75°$.

it can be seen that $\Delta\theta_r/\Delta n_s$ increases with the reduced refractive index of the prism (cos θ_r decreases with an increase of θ_r). Therefore, the high sensitivity of the proposed sensor originates from the combination of the usage of the graphene-MoS_2 hybrid layer and the prism with the low refractive index.

4. CONCLUSIONS

In conclusion, the performance of the SPR biosensor based on a graphene-MoS_2 hybrid structure with MgF_2 prism has been numerically investigated. With the adjustment of the parameters in the proposed configuration, we can obtain an ultrasensitive and high figure-of-merit SPR biosensor, and the value of sensitivity is as high as 540.8°/RIU. The introduction of the MgF_2 prism with low refractive index and the graphene-MoS_2 hybrid layer largely affects the distribution of the field in the sensing region and then enhances the performance of the biosensor. The proposed structure may provide a new way for designing ultrasensitive SPR biosensors.

Funding. Jiangsu Innovation Program for Graduate Education (KYZZ16_0167); China Scholarship Council (CSC).

Acknowledgment. Yuncai Feng wants to acknowledge the financial support from the CSC.

REFERENCES

1. S. A. Maier, *Plasmonics: Fundamentals and Applications* (Springer 2007).
2. S. Zeng, S. Hu, J. Xia, T. Anderson, X. Q. Dinh, X. M. Meng, P. Coquet, and K. T. Yong, "Graphene-MoS_2 hybrid nanostructures enhanced surface plasmon resonance biosensors," Sens. Actuators B **207**, 801–810 (2015).
3. P. K. Maharana, R. Jha, and P. Padhy, "On the electric field enhancement and performance of SPR gas sensor based on graphene for visible and near infrared," Sens. Actuators B **207**, 117–122 (2015).
4. L. Wu, H. S. Chu, W. S. Koh, and E. P. Li, "Highly sensitive graphene biosensors based on surface plasmon resonance," Opt. Express **18**, 14395–14400 (2010).
5. H. Xu, L. Wu, X. Dai, Y. Gao, and Y. Xiang, "An ultra-high sensitivity surface plasmon resonance sensor based on graphene-aluminum-graphene sandwich-like structure," J. Appl. Phys. **120**, 053101 (2016).
6. T. Srivastava and R. Jha, "Black phosphorus: a new platform for gaseous sensing based on surface plasmon resonance," IEEE Photon. Technol. Lett. **30**, 319–322 (2018).
7. P. K. Maharana, T. Srivastava, and R. Jha, "Low index dielectric mediated surface plasmon resonance sensor based on graphene for near infrared measurements," J. Phys. D **47**, 385102 (2014).
8. L. Wu, J. Guo, H. Xu, X. Dai, and Y. Xiang, "Ultrasensitive biosensors based on long-range surface plasmon polariton and dielectric waveguide modes," Photon. Res. **4**, 262–266 (2016).
9. Z. Lin, L. Jiang, L. Wu, J. Guo, X. Dai, Y. Xiang, and D. Fan, "Tuning and sensitivity enhancement of surface plasmon resonance biosensor with graphene covered Au-MoS 2-Au Films," IEEE Photon. J. **8**, 4803308 (2016).
10. A. Lahav, M. Auslender, and I. Abdulhalim, "Sensitivity enhancement of guided-wave surface-plasmon resonance sensors," Opt. Lett. **33**, 2539–2541 (2008).
11. P. K. Maharana, T. Srivastava, and R. Jha, "Ultrasensitive plasmonic imaging sensor based on graphene and silicon," IEEE Photon. Technol. Lett. **25**, 122–125 (2013).
12. Z. Lin, Y. Jia, Q. Ma, L. Wu, B. Ruan, J. Zhu, X. Dai, and Y. Xiang, "High sensitivity intensity-interrogated Bloch surface wave biosensor with graphene," IEEE Sens. J. **18**, 106–110 (2017).
13. R. Verma, B. D. Gupta, and R. Jha, "Sensitivity enhancement of a surface plasmon resonance based biomolecules sensor using graphene and silicon layers," Sens. Actuators B **160**, 623–631 (2011).
14. Q. Ouyang, S. Zeng, L. Jiang, L. Hong, G. Xu, X. Q. Dinh, J. Qian, S. He, J. Qu, P. Coquet, and K. T. Yong, "Sensitivity enhancement of transition metal dichalcogenides/silicon nanostructure-based surface plasmon resonance biosensor," Sci. Rep. **6**, 28190 (2016).
15. A. H. C. Neto, "The electronic properties of graphene," Phys. Status Solidi **83**, 1248–1252 (2007).
16. H. J. Li, L. L. Wang, J. Q. Liu, Z. R. Huang, B. Sun, and X. Zhai, "Investigation of the graphene based planar plasmonic filters," Appl. Phys. Lett. **103**, 211104 (2013).
17. Y. Feng, Y. Liu, X. Wang, D. Dong, Y. Shi, and L. Tang, "Tunable multichannel plasmonic filter based on a single graphene sheet on a Fibonacci quasiperiodic structure," Plasmonics **13**, 653–659 (2018).
18. M. Liu, X. Yin, E. Ulin-Avila, B. Geng, T. Zentgraf, L. Ju, F. Wang, and X. Zhang, "A graphene-based broadband optical modulator," Nature **474**, 64–67 (2011).
19. Y. Feng, Y. Liu, Y. Shi, X. Wang, and D. Dong, "An ultra-compact tunable intersection structure based on graphene nanoribbon," J. Phys. D **50**, 185101 (2017).
20. B. Wang, X. Zhang, X. Yuan, and J. Teng, "Optical coupling of surface plasmons between graphene sheets," Appl. Phys. Lett. **100**, 131111 (2012).
21. Y. Shao, J. Wang, H. Wu, J. Liu, I. A. Aksay, and Y. Lin, "Graphene based electrochemical sensors and biosensors: a review," Electroanalysis **22**, 1027–1036 (2010).
22. P. K. Maharana and R. Jha, "Chalcogenide prism and graphene multilayer based surface plasmon resonance affinity biosensor for high performance," Sens. Actuators B **169**, 161–166 (2012).
23. L. Wu, J. Guo, X. Dai, Y. Xiang, and D. Fan, "Sensitivity enhanced by MoS_2–graphene hybrid structure in guided-wave surface plasmon resonance biosensor," Plasmonics **13**, 281–285 (2017).
24. L. Wu, J. Guo, Q. Wang, S. Lu, X. Dai, Y. Xiang, and D. Fan, "Sensitivity enhancement by using few-layer black phosphorus-graphene/TMDCs heterostructure in surface plasmon resonance biochemical sensor," Sens. Actuators B **249**, 542–548 (2017).

25. L. Wu, Y. Jia, L. Jiang, J. Guo, X. Dai, Y. Xiang, and D. Fan, “Sensitivity improved SPR biosensor based on the MoS_2/graphene–aluminum hybrid structure,” J. Lightwave Technol. **35**, 82–87 (2017).
26. A. K. Mishra and S. K. Mishra, “MgF_2 prism/rhodium/graphene: efficient refractive index sensing structure in optical domain,” J. Phys. Condens. Matter **29**, 145001 (2017).
27. P. K. Maharana, R. Jha, and S. Palei, “Sensitivity enhancement by air mediated graphene multilayer based surface plasmon resonance biosensor for near infrared,” Sens. Actuators B **190**, 494–501 (2014).
28. C. W. Lin, K. P. Chen, C. N. Hsiao, S. Lin, and C. K. Lee, “Design and fabrication of an alternating dielectric multi-layer device for surface plasmon resonance sensor,” Sens. Actuators B **113**, 169–176 (2006).
29. G. Ghosh, *Handbook of Optical Constants of Solids* (Academic, 1998).
30. M. Bruna and S. Borini, “Optical constants of graphene layers in the visible range,” Appl. Phys. Lett. **94**, 031901 (2009).
31. A. Castellanos-Gomez, N. Agraït, and G. Rubio-Bollinger, “Optical identification of atomically thin dichalcogenide crystals,” Appl. Phys. Lett. **96**, 213116 (2010).
32. M. Daimon and A. Masumura, “Measurement of the refractive index of distilled water from the near-infrared region to the ultraviolet region,” Appl. Opt. **46**, 3811–3820 (2007).
33. W. Lee and D. Kim, “Field-matter integral overlap to estimate the sensitivity of surface plasmon resonance biosensors,” J. Opt. Soc. Am. A **29**, 1367–1376 (2012).